Lasers in Medical Science
https://doi.org/10.1007/s10103-020-03128-6

ORIGINAL ARTICLE

A novel technique for laser-assisted revascularization: an in vitro pilot study

Zacharia Mbaidjol[1] · Michael H. Stoffel[2] · Martin Frenz[3] · Mihai A. Constantinescu[1]

Received: 25 January 2020 / Accepted: 10 August 2020

Abstract

The common limitation of surgical revascularization procedures for severe tissue ischemia due to cardiovascular diseases is the need to interrupt blood flow during the intervention. We aim to introduce a new technique that allows a sutureless, non-occlusive revascularization. A 3-step technique was developed using rabbit's aorta to simulate a side-to-side anastomosis model. It enables the creation of a bypass circuit for revascularization. The first step was the soldering of 2 vessels in a side-to-side fashion based on the laser-assisted vascular anastomosis (LAVA) principle using a diode laser emitting irradiation at 810 nm with an albumin-based solder patch between them, followed by the creation of a channel within the patch using either a holmium-doped yttrium aluminum garnet laser (Ho:YAG) at λ = 2100 nm or a xenon-chloride excimer laser (XeCl) at λ = 308 nm. Thereby, a bypass circuit was created, thus allowing a non-ischemic revascularization. The system was deemed functional when a flow was observed across the anastomosis. The highest average tensile strength recorded after side-to-side LAVA using a diode laser power of 3.2 W for 60 s was 2278.6 ± 800 mN (n = 20). The Ho:YAG laser created the channels with less tension on the anastomosis than the excimer laser. Histological analysis showed limited thermal damage and good patch-tissue adaptation. The preliminary results of this feasibility study outline the foundations for an entirely sutureless laser-assisted revascularization procedure. The next studies will evaluate the rheological parameters across the bypass circuit to optimize the post-anastomotic flow.

Keywords Blood flow · Bypass surgery · Tissue soldering · Albumin patch · Side-to-side anastomosis · Sutureless

Introduction

Cardiovascular diseases (CVD) are the number one cause of death globally [1]. It accounts for an underlying cause of death for around 1 in every 7 deaths in the USA in 2011 [2] and peripheral artery disease (PAD) is expected to cause between 500 and 1000 new cases of critical limb ischemia every year per million habitants in North America and Europe [3]. In many cases, revascularization through a bypass of the severely occluded arterial segment is the only possible treatment option. Vascular bypass surgery's use is however not limited to peripheral revascularization and cardiovascular heart disease (CHD). The same principles are applied to extracranial-intracranial (EC-IC) bypass surgery for the treatment of stroke caused by symptomatic occlusion of the internal carotid artery [4].

The technique for the surgical treatment of severe vascular pathologies has strongly improved since Alexis Carrel and Charles Guthrie [5] first described the use of a vein to bypass an arterial segment at the beginning of the last century. One common important limitation during these major surgeries however is the prolonged ischemia needed in order to successfully perform the revascularization. Research towards techniques, which allow to avoid or reduce ischemia during bypass surgery, is a logical consequence. In neurosurgery, Tulleken et al. established the ELANA technique (excimer laser-assisted non-occlusive anastomosis) [6] allowing to perform EC-IC bypass without inducing further ischemia to the already hypo-perfused brain. This two-step side-to-end

✉ Zacharia Mbaidjol
zahqaria@gmail.com

1 Department of Plastic and Reconstructive Surgery, University Hospital Bern, Freiburgstrasse, 3010 Bern, Switzerland

2 Division of Veterinary Anatomy, University of Bern, Länggass-Strasse 120, CH-3001 Bern, Switzerland

3 Department of Biomedical Photonics, Institute of Applied Physics, University of Bern, Sidlerstrasse 5, 3012 Bern, Switzerland

Published online: 19 August 2020

procedure includes the suturing of the donor vessel to the still perfused recipient vessel using a platinum ring at the interface and the subsequent perforation of the vessel wall using an excimer laser.

What is known of the potency of laser irradiation on vascular tissue comes mostly from clinical histopathological and animal studies. The structural damages inflicted to the vessel and the healing time depend on the power used, the specificity of the laser, and the duration of the irradiation [7, 8]. Factors intrinsic to the vessel are also to be taken into consideration [9]. The major risk of laser irradiation to the vascular tissue is caused by overheating and range from coagulation thrombosis to a full necrosis [10]. But compared with conventional suture repair, laser irradiation seemed to cause less scar tissue and less tissue reaction due to the absence of foreign body [11].

It is also suggested that laser non-ionizing radiation causes deleterious effects to the target organ at a molecular and cellular level depending on the laser intensity used. Low-level laser irradiation has been shown to increase DNA damages and reduce cell viability in a dose-depending manner through gene transcription, intracellular signaling, and protein regulation on a human umbilical vein endothelial cell model. This is not without consequences as it could accordingly reduce the neovascular potential of the vessel [12].

We present in this article a side-to-side laser-assisted revascularization technique in vitro that allows a sutureless, non-ischemic revascularization. This method enables a prompt restoration of the blood flow without the necessity to interrupt the main blood stream in the bypassed vessel. The aim of this study is to evaluate the feasibility of this new technique.

Materials

The laser-assisted revascularization technique consists of 3 steps. The first step is the side-to-side soldering of the donor and recipient vessel, followed by the creation of channels perforating the soldered vessel walls and finally the design of a functional bypass circuit.

Preparation of the soldering material

The solder patch

The solder patch was produced by electrospinning [12]. In brief, a polycaprolactone (PCL)/indocyanine green (ICG) solution was prepared by dissolving separately PCG (Sigma-Aldrich Saint Louis, MO) and ICG (Acros Organics Geel, Belgium) in a chloroform/methanol (75/25% v/v) (Merck KGaA Darmstadt, Germany) solution and stirring them overnight. Both solutions were then combined to obtain a 9% wt. PCL solution with an ICG ratio of 1:10. The combined solution was loaded into a 5-ml syringe with a truncated needle (0.812 mm I.D.), which was connected to a high voltage power supply. For electrospinning, a positive potential of 15 kV between the needle and the collector was used. The solution was pumped with a flow rate of 30 μl/min. The fibers were collected on a grounded rotating aluminum collector plate located at a distance of 15 cm.

The bovine serum albumin solution

The liquid protein solution was prepared by dissolving 40% (w/w) bovine serum albumin in ultrapure water. It was then magnetically stirred overnight at 37 °C.

Before use, the electrospun PCL/ICG patches were fully soaked in the bovine serum albumin (BSA) solution. They were left to dry at room temperature for 20 min, then cut to a size of 5 mm width by 10 mm length and sealed in small plastic bags with a commercially available vacuum sealer.

Rabbit aortas

Rabbit aortas were obtained from a local butcher (Kani-Swiss GmbH, Geltwil, Switzerland) and were stored within 2 h after slaughtering at − 80 °C. Prior to use, they were defrosted at room temperature for 1 h.

Methods

The experiments were performed between November 2016 and February 2018 at the Institute of Applied Physics in Bern and the research facility of the Plastic Surgery Department at the Inselspital in Bern.

First step: soldering

The aortas were prepared on a length of 6 cm and the vessels were cut into 2 segments of equal length. The two segmented vessels were then each mounted on a percutaneous angioplasty (PTA) balloon catheters of 3 mm diameter placed in parallel to each other (Armada 35 PTA catheter, Abbott Laboratories, Illinois). Two soldering patches were placed between the 2 vessels, one at 1 cm from the left extremity and the other at 1 cm from the right extremity. The balloon catheters were thereafter inflated with a saline solution. This allowed to maintain the 2 vessels in close contact. A custom-made laser fiber (diameter of 0.8 mm) with a light diffuser at its distal end (cylindrical light diffuser, model RD, Medlight SA, Ecublens, Switzerland) was introduced through the working channel of the PTA catheter in the top vessel (donor vessel). Precise positioning of the fiber at the level of the patch was verified with a target laser beam. The 2 vessel stumps were kept in place with the use of a microvascular surgical clamp (Acland approximator clamp, Synovis Micro Companies Alliance Inc., Birmingham, USA) placed at the anastomosis site. Once the positioning of the two vessels was completed, the soldering process was performed with a diode laser (Lina 30d, Intros, Heilbad Heiligenstadt, Germany) emitting irradiation at 810 nm. During the soldering process, the temperature profile at the top of the donor vessel was recorded with a Thermo-camera (A655, FLIR System, Inc., Wilsonville, Oregon). The energy emitted from the laser was also recorded. The same procedure was performed to fuse the two vessels at the position of the second patch by moving the laser fiber within the lumen (Fig. 1)

Two different soldering powers were evaluated: 2.8 W and 3.2 W at 2 soldering irradiation times: 45 s and 60 s. At 2.8 W, we additionally evaluated soldering with 75 s duration to assess the effect of the combination of low irradiation and long irradiation duration on the anastomosis tensile strength. Samples were then either used for the second step of the experiment or stored in 4% formaldehyde solution (G256, Dr. Grogg Chemie AG, Stettlen, Switzerland) for histology to assess the thermal effects, or they were prepared for tensile strength assessment.

Second step: perforation (creation of channels)

In order to create the anastomosis, 2 different laser sources were compared. The recipient vessel (lower vessel) was mounted on an automatic perfusor (Perfusor FM Pump IV Infusion, Braun, Aschaffenburg, Germany) that maintained a constant pre-determined flow of 100 ml/min of saline solution (Inselspital, Bern, Switzerland). Collateral vessel branches were cauterized to avoid any leakage. A laser fiber of core diameter 600 μm (Calculase II Karl Storz, Tuttlingen, Germany) was introduced in the lumen of the donor vessel through one extremity. The laser beam was aimed at the ipsilateral patch with a slight contact against the vessel wall. The perforation was performed using a holmium-doped yttrium aluminum garnet laser (Ho:YAG) at a wavelength of λ = 2100 nm with a repetition rate of 4 Hz, a pulse duration of 300 μsec, and a pulse energy of 800 mJ.

The same procedure was then repeated on the other end of the graft vessel to create a channel in the contralateral patch.

The second laser used was an excimer laser λ = 308 nm (CVX-300, Spectranetics, Zug, Switzerland) with a fiber specifically designed for ELANA procedures in extracranial-intracranial (EC-IC) bypass surgery (ELANA catheter 2.0, Ultrecht, Netherlands). Again, the fiber was introduced from both sides of the donor vessel and drilling was performed until a channel was created with a power of 40 mJ/mm^2 and 40 pulses or until flow was observed across the system.

Third step: evaluation of the bypass system

To evaluate the functionality of the circuit, the recipient vessel was ligated in the middle with medium Ligaclips (Ethicon US. LLC, OH, USA) in order to mimic a full circumferential thrombose. Both ends of the donor vessels were also ligated. The bypass system was considered functional when a flow was observed across the anastomosis from the proximal end of the silicone tube to the distal end.

Tensile strength measurements

Tensile strength was assessed using a test stand with a fixed force gauge (BFG50, Mecmesin Limited, West Sussex, UK). The 2 vessels were fixed on custom-made supports, which were attached to a moving table. The table was electrically moved at a constant velocity of 30 mm/min. Measurements were all performed at the latest 4 min after soldering perpendicular to the vessel. The tensile strength at the breaking point was recorded in millinewtons for a total of 118 vessels.

Histological analysis

Paraffin embedding was done according to standard protocols [13]. Thereafter, samples were dehydrated in an ascending ethanol series (70%, 80%, 90%, 94%, 100% vol/vol for 20 min each) and embedded in Epon resin, a mixture of Epoxy embedding medium, dodecenyl succinic anhydride (DDSA), and methyl nadic anhydride (MNA) (Sigma-Aldrich, Buchs, Switzerland). Semi thin sections of 0.5 μm were obtained with diamond knives (Diatome, Biel, Switzerland) on a Reichert-Jung Ultracut E (Leica, Heerbrugg, Switzerland) and stained with toluidine blue.

Statistical analysis

Statistical analysis was performed using SPSS (IBM Corp. released 2012. IBM SPSS Statistics for Windows, version 21.0. Armonk, NY: IBM Corp). Unpaired T test was carried out. Values were given as mean ± standard deviation and statistical significance was given to values with $p < 0.05$.

Results

We were able to carry out the first 2 steps of the bypass circuit with no difficulty according to the protocol due to our previous experience with the LAVA technique. None of our specimens sustained any perforation throughout the soldering

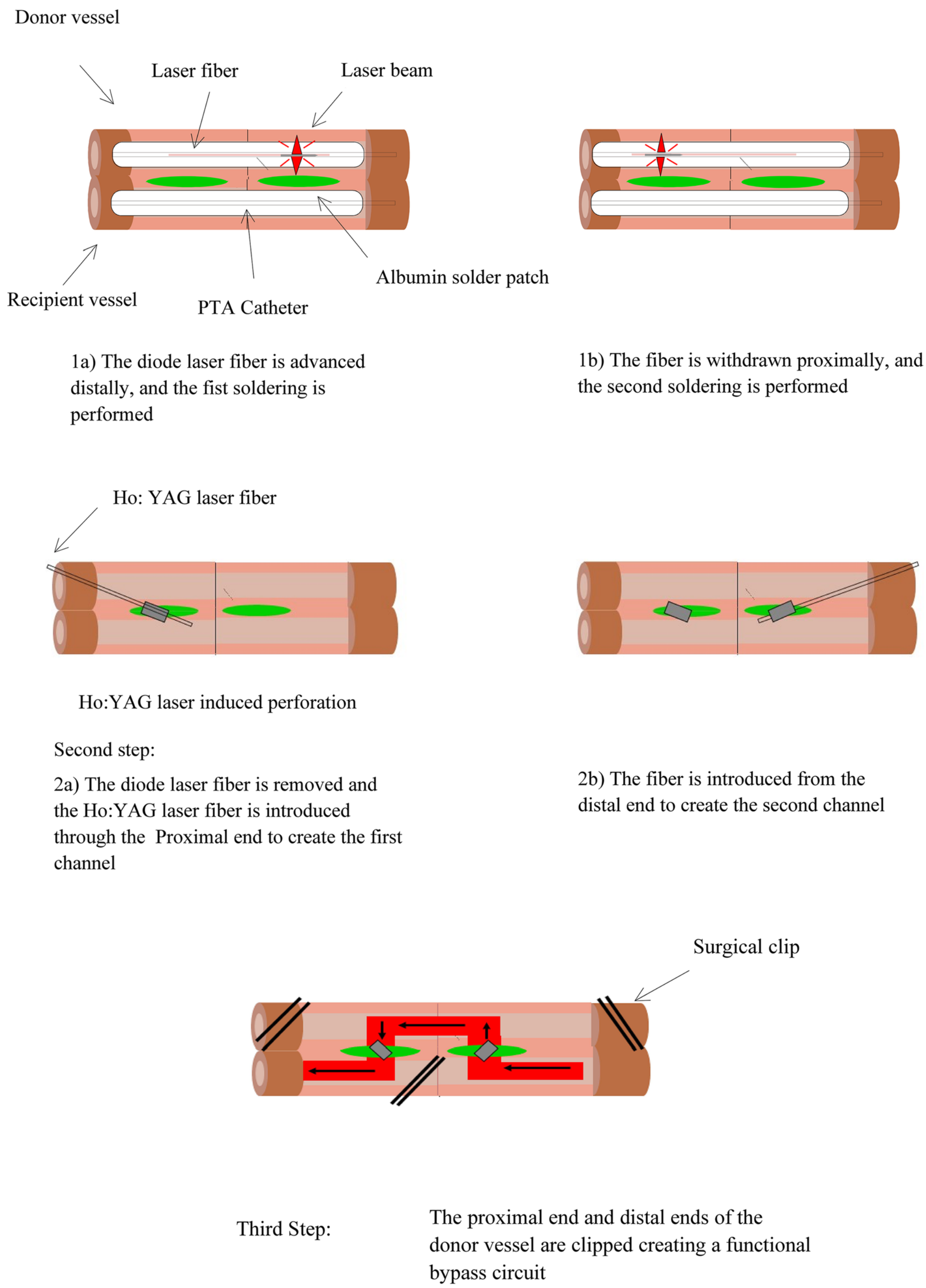

Fig. 1 Schematic of the 3 steps to create the bypass circuit

process. The samples showed uniform soldering and the tearing location at the anastomosis site could not be predicted before tensile strength measurements. The highest average values were recorded with a power of 3.2 W for 60 s at 2278.6 ± 800 mN ($n = 20$) (Fig. 2). Keeping the laser power constant, the tensile strength increased when increasing the irradiation time ($p < 0.32$) (Fig. 2). For the perforation step, a steep learning curve was first necessary to know how to guide the catheter across the anastomosis. We thereafter had no catheter-induced perforation. Gentle pressure was applied to the fiber until it pierced into the lumen of the recipient vessel. Successful drilling was confirmed when the laser fiber could be freely advanced into the recipient vessel's lumen.

During soldering, the increase in temperature varied with the laser power used and the duration of soldering. The highest average temperature was recorded with a power of 3.2 W and a duration of 60 s (Table 1).

Light microscopical analysis of the soldered specimens at 3.2 W and 60 s showed a good adaptation of the solder to the vessel wall and unaltered appearance of the vessel wall (Fig.

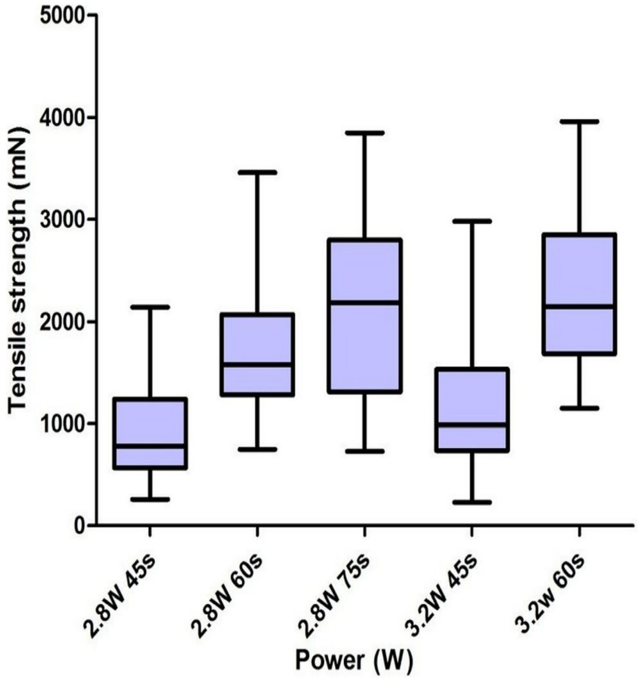

Fig. 2 Tensile strength measurements according to the different power and duration investigated. The boxes indicate the median and interquartile range. The upper and lower horizontal bars represent the maximum and minimum obtained values

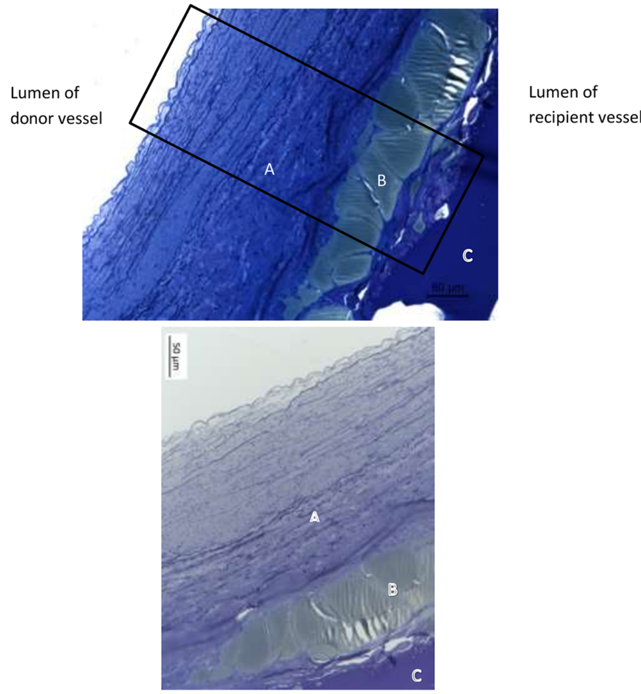

Fig. 3 Toluidine blue staining after soldering with a power of 3.2 W for 60 s. The intact structure of the donor arterial wall is depicted. The elastic fibers can be distinguished in the arterial wall (A), as well as some residual adipose tissues in the adventitia (B). The patch can be recognized by its characteristic amorphous aspect (C)

3). These parameters were therefore selected for the rest of the experiment. With an irradiation of 2.8 W for 75 s, the mean tensile strength and the highest values were comparable with the highest obtained values at 3.2 W and 60 s, but the tissue had macroscopically evident thermal damages as opposed to the group at 3.2 W and 60 s. Further analyses with these settings were therefore discontinued.

No leaks were observed during the evaluation of the bypass system and a flow was observed across the circuit (Figs. 4 and 5). This enabled us to show that the anastomosis could withstand a flow of 100 ml/min. We did not attempt to measure the pre-and post-anastomotic flow as this will be subject to further studies in a compliant aortic root model [14].

Table 1 Temperature recorded at the top surface of the donor vessel during laser soldering

	2.8 W 45 s	2.8 W 60 s	2.8 W 75 s	3.2 W 45 s	3.2 W 60 s
N	25	19	24	26	24
Average T (°C)	93.3	99.8	101.5	92.5	110.6
SD	10.5	12.7	19.4	9.85	17.78
Maximum	125	125	160	117	158
Minimum	77	73	70	78	72
Energy (Joules)	126	168	210	144	192

Discussion

The use of an extracorporeal circuit as it is currently used during bypass surgery has been shown to increase the formation of reactive oxygen and proinflammatory species during surgery [15]. This in vivo study is a first step towards the development of a sutureless non-ischemic bypass surgery. We previously showed that laser-assisted vascular surgery allowed successful end-to-end anastomosis in a pig model [9].

During the first step of our experiments, we obtained the maximal tensile strength with a power of 3.2 W and irradiation duration of 60 s as this duration allows the denaturation of the protein of the solder [16]. Lower values were obtained with shorter irradiation times. Though the temperature measurements recorded do not represent the intraluminal temperature as they were recorded on the surface of the anastomosis, the lowest average temperature was recorded with the shortest duration of irradiation. One can assume that with a power of 2.8 W despite reaching the required temperature for soldering, the duration of irradiation was not sufficient to create a strong scaffold. On the other hand, with a lower irradiation power (2.8 W) for a long duration (75 s), the maximum temperature and energy used were recorded and macroscopic damages to the vessels were obvious. This is in contrast to 3.2 W with 60 s duration where the highest average temperature was recorded but damages to the vessel were only apparent on histology. This implies

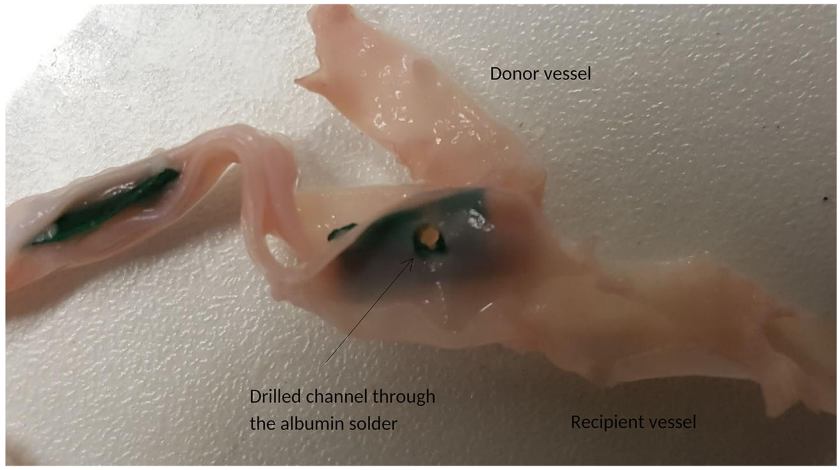

Fig. 4 View of the posterior wall of the recipient vessel following soldering with a diode laser (3.2 W for 60 s) and perforation with an excimer laser (40 mJ/mm^2 with 40 pulses). The vessel is opened longitudinally to visualize the channel created

that other factors such as the humidity of the vessel and the thickness of the vessel wall probably influence the absorption of energy and the temperature of the system. Further studies are needed to determine the maximal tolerated energy and temperature before structural damages are observed on the vessel wall.

The second step of the procedure consisted of a laser-induced perforation of the solder fixed to the vessel wall on both sides. Laser ablation and vaporization of vascular tissue have been described since 1982 [17, 18] and have been successfully used for the revascularization of coronary vessels and peripheral vessels [19, 20] with various laser sources. Regardless of the laser used, the goal is to ablate atheromatous plaques and promptly restore blood flow while creating minimal debris and minimal damages to the vessel wall.

Great interest has been given to the use of holmium laser because of its important absorption by water and its ability to ablate tissue with reduced damages to surrounding tissue [21]. It operates in a pulsed mode in the near-infrared area of the electromagnetic spectrum at a wavelength of 2100 nm not far from the absorption peak of water which is at 1.94 um. Holmium laser can also easily be coupled into an OH-fused silica fiber and can then be fitted in a guiding catheter. Furthermore, holmium laser irradiation coupled into a fiber can ablate tissue both in contact and non-contact mode [22].

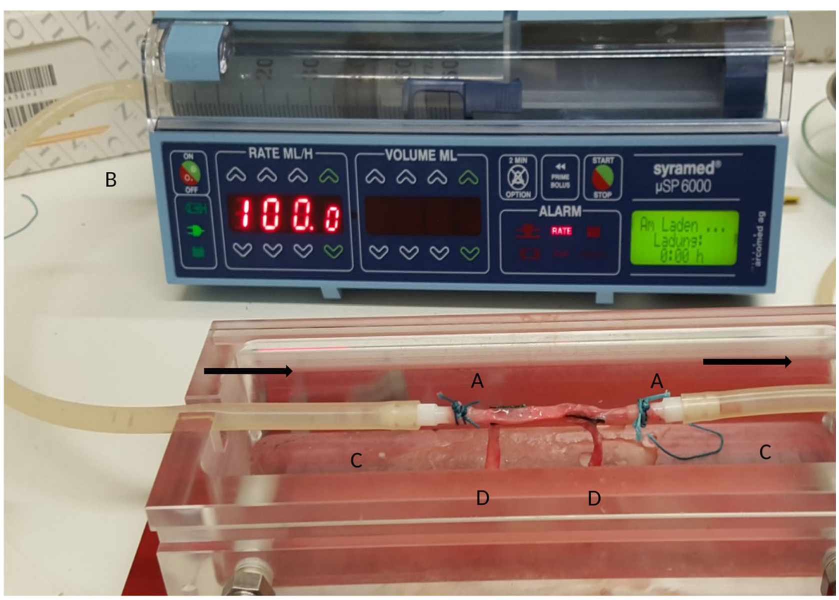

Fig. 5 Experimental setup simulating the final step of the bypass circuit after soldering with a diode laser (3.2 W for 60 s) and the creation of the channels with a Ho:YAG laser (4 Hz, pulse duration of 300 µsec, pulse energy of 800 mJ). A ligature was placed in the center of the recipient vessel (A) to simulate an obstacle (not visible on the picture). An automated perfusor (B) attached via two silicone tubes (C) to the two extremities of the recipient vessel allowed a continuous flow across the anastomosis from the proximal tube to the distal one. The donor vessels can be seen soldered to the recipient vessel, hanging down due to gravity (D). No leakage was observed. The arrow indicates the direction of flow of the saline solution from the automated perfusor across the anastomosis

The particularity with our setting resides in the fact that 2 layers of endothelium and a patch have to be ablated in order to create a channel between the 2 vessels. In contact mode, the water content in the vessel wall acts as a chromophore for the photon, thus strongly absorbing the energy and allowing tissue vaporization. Furthermore, Kopchok et al. [7] showed that in the contact mode, the thermal injury to adjacent tissue was also determined by the applied force for tissue penetration and the pulse width.

With this setting, the vessel walls were vaporized and the fiber went through with no difficulty. We observed a subtle resistance as the patch was ablated; the fiber went then almost simultaneously through the second vessel wall. Care had to be taken not to induce a vessel perforation by withdrawing the fiber directly after perforation of the vessel wall. We were not able in this study to determine the ideal drilling parameters due to the high variation among the tested specimens (water content, thickness). To confirm ex vivo the successful creation of the channels, the laser fiber was freely advanced in the lumen of the recipient vessel and the laser beam could also be visualized in the recipient vessel.

Histological analysis showed structural and architectural damages in the vicinity from the anastomosis and the outer vessel wall. During the ablation procedure, we did not evaluate the size of the residual debris after ablation as this was not the aim of this study. This is not a negligible issue as debris of considerable size may cause pulmonic embolism. Having the vessels connected to an automated perfusor with saline solution allowed us to show the functionality of the bypass circuit.

The ELANA technique [23] is a non-occlusive surgical technique used in neurosurgery for revascularization procedures. It also enables the creation of vascular anastomoses through vessel ablation with an excimer laser (wavelength 308 nm). With this technique, the recipient and donor vessels are held in contact through a custom-made ring sutured between the two vessels. Irradiation is performed with a laser fiber which consists of a bundle of fibers. It conducts the energy to the vessel wall and cuts a hole, thereby creating a functional anastomosis. A firm contact between the vessel wall and the fiber is required in order for the process to take place. Hence, in order to position the laser fiber in the lumen of the donor vessel perpendicular to the recipient vessel, an increased amount of tension had to be applied on the newly created anastomosis making it prompt to failure. We were nevertheless able to successfully create channels through the solder with the excimer laser, but the use of a holmium fiber would be a solution to this problem allowing less stress and risk of leakage to the anastomosis.

Potential complications associated with our new technique are inherent to the use of laser and revascularization procedures and will need to be investigated. Adequate control of the temperature during soldering has always been a major concern in order to avoid heat-associated damages to the vessel and will need to be addressed. Furthermore, the risk of major adverse postoperative events such as thrombosis, vessel dissection, or rupture and the risk of embolus will also need more assessment.

Conclusion

This study is a first step towards creating an entirely sutureless laser-assisted revascularization procedure while simultaneously avoiding the prolonged ischemia induced with current standard techniques. Further studies will focus on the assessment of the debris created during the ablation process and on how to reduce the laser-induced damages to the vessel. The rheological parameters across the bypass circuit will also need to be assessed to optimize the post-anastomotic flow.

Acknowledgments The authors would like to thank Annemarie Schönfeld for her help with this project.

Funding information This study was supported by a grant of the Swiss National Science Foundation (project number 108447).

Compliance with ethical standards

Conflict of interest The authors declare that they have no conflict of interest.

Ethical approval Not applicable.

Informed consent This article does not contain any studies with human participants performed by any of the authors.

References

1. Mendis S, Davis S, Norrving B (2015) Organizational update: the world health organization global status report on noncommunicable diseases 2014; one more landmark step in the combat against stroke and vascular disease. Stroke 46(5):e121–e122. https://doi.org/10.1161/STROKEAHA.115.008097
2. Mozaffarian D, Benjamin EJ, Go AS, Arnett DK, Blaha MJ, Cushman M, de Ferranti S, Despres JP, Fullerton HJ, Howard VJ, Huffman MD, Judd SE, Kissela BM, Lackland DT, Lichtman JH, Lisabeth LD, Liu S, Mackey RH, Matchar DB, DK MG, Mohler ER 3rd, Moy CS, Muntner P, Mussolino ME, Nasir K, Neumar RW, Nichol G, Palaniappan L, Pandey DK, Reeves MJ, Rodriguez CJ, Sorlie PD, Stein J, Towfighi A, Turan TN, Virani SS, Willey JZ, Woo D, Yeh RW, Turner MB, American Heart Association Statistics C, Stroke Statistics S (2015) Heart disease and stroke statistics-2015 update: a report from the American Heart Association. Circulation 131(4):e29–e322. https://doi.org/10.1161/CIR.0000000000000152
3. Norgren L, Hiatt WR, Dormandy JA, Nehler MR, Harris KA, Fowkes FG, Group TIW (2007) Inter-society consensus for the management of peripheral arterial disease (TASC II). J Vasc Surg 45(Suppl S):S5–S67. https://doi.org/10.1016/j.jvs.2006.12.037

4. Donaghy RMP, Yasargil MG (1967) Experimental small vascular surgery in the dog including patching and grafting of cerebral vessels and the formation of functional extra-intracranial shunts. Microvasc Surg:87–126
5. Carrel A (1910) VIII. On the experimental surgery of the thoracic aorta and heart. Ann Surg 52(1):83–95
6. ter Berg JW, Dippel DW, Habbema JD, Westermann CJ, Tulleken CA, Willemse J (1993) Unruptured intracranial arteriovenous malformations with hereditary haemorrhagic telangiectasia. Neurosurgical treatment or not? Acta Neurochir 121(1-2):34–42
7. Kopchok GE, White RA, Tabbara M, Saadatmanesh V, Peng SK (1990) Holmium:YAG laser ablation of vascular tissue. Lasers Surg Med 10(5):405–413
8. Puca A, Esposito G, Albanese A, Maira G, Rossi F, Pini R (2009) Minimally occlusive laser vascular anastomosis (MOLVA): experimental study. Acta Neurochir 151(4):363–368; discussion 368. https://doi.org/10.1007/s00701-009-0219-3
9. Mbaidjol Z, Kiermeir D, Schonfeld A, Arnoldi J, Frenz M, Constantinescu MA (2017) Endoluminal laser-assisted vascular anastomosis-an in vivo study in a pig model. Lasers Med Sci 32(6):1343–1348. https://doi.org/10.1007/s10103-017-2250-6
10. McKenzie AL (1986) A three-zone model of soft-tissue damage by a CO2 laser. Phys Med Biol 31(9):967–983. https://doi.org/10.1088/0031-9155/31/9/003
11. Gelli R, Pini R, Toncelli F, Chiarugi C, Reali UM (1997) Vessel-wall recovery after diode laser-assisted microvascular anastomosis: clinical and histologic analysis on long-term follow-up. J Reconstr Microsurg 13(3):199–205. https://doi.org/10.1055/s-2007-1006405
12. Schonfeld A, Kabra ZM, Constantinescu M, Bosshardt D, Stoffel MH, Peters K, Frenz M (2017) Binding of indocyanine green in polycaprolactone fibers using blend electrospinning for in vivo laser-assisted vascular anastomosis. Lasers Surg Med 49(10):928–939. https://doi.org/10.1002/lsm.22701
13. Mulisch M, Welsch U (2015) (eds.). Romeis Mikroskopische Technik. 19th ed. Berlin, Heidelberg: Springer Spektrum
14. Jahren SE, Heinisch PP, Wirz J, Winkler BM, Carrel T, Obrist D (2015) Hemodynamic performance of Edwards Intuity valve in a compliant aortic root model. Conf Proc IEEE Eng Med Biol Soc 2015:3315–8. https://doi.org/10.1109/EMBC.2015.7319101
15. Devanathan V, Hagedorn I, Kohler D, Pexa K, Cherpokova D, Kraft P, Singh M, Rosenberger P, Stoll G, Birnbaumer L, Piekorz RP, Beer-Hammer S, Nieswandt B, Nurnberg B (2015) Platelet Gi protein Galphai2 is an essential mediator of thrombo-inflammatory organ damage in mice. Proc Natl Acad Sci U S A 112(20):6491–6496. https://doi.org/10.1073/pnas.1505887112
16. Parrish JA, Anderson RR, Harrist T, Paul B, Murphy GF (1983) Selective thermal effects with pulsed irradiation from lasers: from organ to organelle. J Invest Dermatol 80(1 Suppl):75s–80s. https://doi.org/10.1038/jid.1983.19
17. Abela GS, Normann S, Cohen D, Feldman RL, Geiser EA, Conti CR (1982) Effects of carbon dioxide, Nd-YAG, and argon laser radiation on coronary atheromatous plaques. Am J Cardiol 50(6):1199–1205
18. Choy DS, Stertzer S, Rotterdam HZ, Sharrock N, Kaminow IP (1982) Transluminal laser catheter angioplasty. Am J Cardiol 50(6):1206–1208
19. Song MH, Tokuda Y, Ito T (2007) Revival of the side-to-side approach for distal coronary anastomosis. J Cardiothorac Surg 2:2. https://doi.org/10.1186/1749-8090-2-2
20. Kraft F, Schmidt C, Van Aken H, Zarbock A (2015) Inflammatory response and extracorporeal circulation. Best Pract Res Clin Anaesthesiol 29(2):113–123. https://doi.org/10.1016/j.bpa.2015.03.001
21. Haase KK, Baumbach A, Wehrmann M, Duda S, Cerullo G, Ruckle B, Steiger E, Karsch KR (1991) Potential use of holmium lasers for angioplasty: evaluation of a new solid-state laser for ablation of atherosclerotic plaque. Lasers Surg Med 11(3):232–237
22. van Leeuwen TG, van der Veen MJ, Verdaasdonk RM, Borst C (1991) Noncontact tissue ablation by holmium: YSGG laser pulses in blood. Lasers Surg Med 11(1):26–34
23. Tulleken CA, Verdaasdonk RM, Mansvelt Beck HJ (1997) Nonocclusive excimer laser-assisted end-to-side anastomosis. Ann Thorac Surg 63(6 Suppl):S138–S142